Web-based Supplementary Materials for Hierarchical Commensurate and Power Prior Models for Adaptive Incorporation of Historical Information in Clinical Trials

by Brian P. Hobbs, Bradley P. Carlin, Sumithra J. Mandrekar, and Daniel J. Sargent

Web Appendix A

Web Figures 1 and 2 compare the power prior models presented in Subsection 3.3 for fixed $\bar{x_0} = 0$, $\sigma^2 = \sigma_0^2 = \hat{\sigma}_0^2 = 1$ with values of $\bar{x}$ varying by column. Evidence for commensurability among the current and historical datasets is weakest in the first columns and strongest in the fourth columns (identical sample means and variances). Web Figure 1 compares marginal posterior distributions for α_0 derived from the modified power prior (11) (solid) and Ibrahim-Chen (IC) (dashed) power prior under a $Beta(1, 1)$ (uniform) hyperprior. Each graph in the top row shows results for $n = 30$ and $n_0 = 60$, while $n_0 = n = 10^7$ in the bottom row. In all 8 scenarios, (11) places slightly more density on large values of α_0 relative to the IC marginal posterior. Notice that failing to normalize the prior with respect to μ causes the IC posterior to be skewed relative to (11). The figure also clearly elucidates the concern about excessive overattenuation for vague $\pi(\alpha_0)$. The bottom right graph contains posteriors that are *flat* despite very strong evidence for commensurability (10^7 observations with identical sufficient statistics) among the historical and current datasets.

Web Figure 2 show results under the proposed LCPP model (14) used in Section 4, which assumes a $Cauchy(0, 30)$ hyperprior on $\log(\tau)$ and $g^\star(\log(\tau)) = \max(\log(\tau), 1)$. The top row contains marginal posterior (solid) and prior (dashed) distributions for α_0. The prior for α_0 is peaked at 1 and flat for values less than 0.6, which facilitates posteriors that are peaked at 1 when evidence for commensurability is strong and flat when the historical and current data conflict. The bottom row contains marginal posterior distributions for $\log(\tau)$, as well as the fat-tailed $Cauchy(0, 30)$ hyperprior. The graphs show that the posterior for $\log(\tau)$

shrinks to values less than 0 when evidence for commensurability is weak. For commensurate data the posterior is highly right-skewed over very large, positive values of τ, which forces α_0 to be near 1 and facilitates more borrowing. This results in much less overattenutation of consistent historical data, yet facilitates sufficient variance inflation when evidence for commensurability with the current data is weak. Simulations in Section 4 demonstrate that the LCPP is more power for a given Type I error rate when compared to the MPP for Gaussian data.

[Figure 1 about here.]

[Figure 2 about here.]

Web Appendix B

Web Figure 3 contains histograms of the average change in ld tumor sum from baseline for the colorectal cancer data used in Section 5: historical for y_0 (left), $y|Z = 0$ (middle), and $y|Z = 1$ (right). The histograms suggest that assumptions of normality are acceptable. Notice that the histogram for FOLFOX (right) places more mass on smaller values. This suggests that FOLFOX achieved a greater reduction in ld sum on average than the IFL regimen.

[Figure 3 about here.]

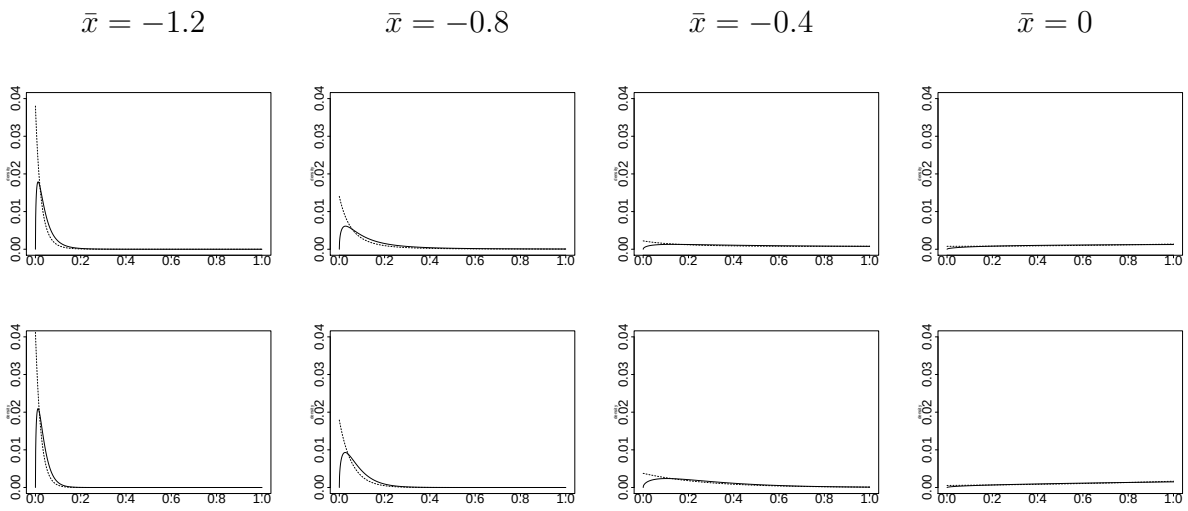

Figure 1. Marginal posterior distributions for α_0 from the MPP (11) (solid) and Ibrahim-Chen (dashed) power prior models under a Beta$(a = 1, b = 1)$ hyperprior, where $\bar{x}_0 = 0$, and fixed $\sigma^2 = \sigma_0^2 = \hat{\sigma}_0^2 = 1$. Each graph in the top row shows results for $n = 30$ and $n_0 = 60$, while $n_0 = n = 10^7$ in the bottom row. Each column corresponds to $\bar{x} = (-1.2, -0.8, -0.4, 0)$.

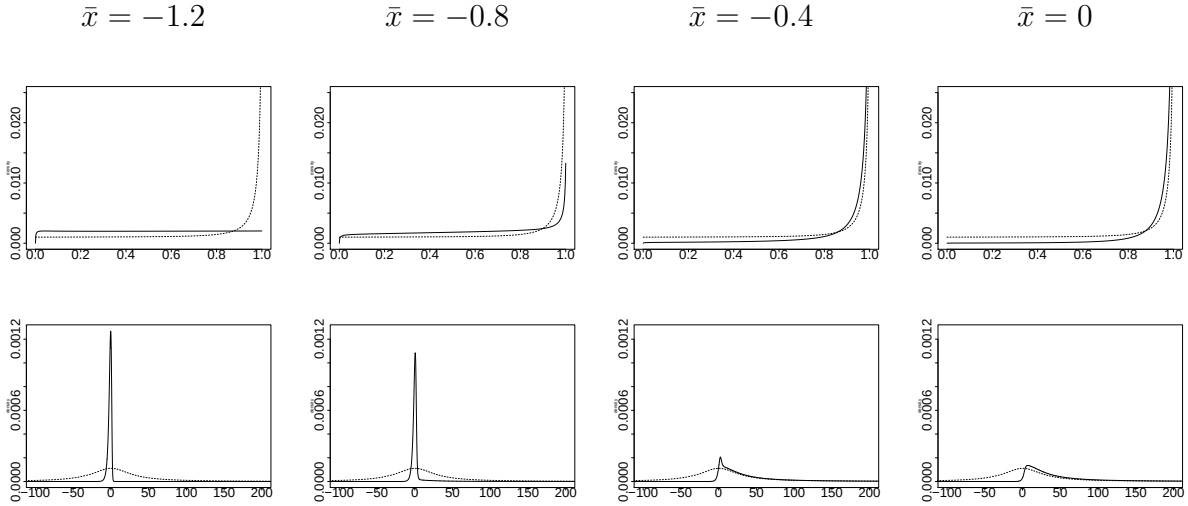

Figure 2. Marginal posterior (solid) and prior (dashed) distributions for α_0 and $\log(\tau)$ under the LCPP (14) used in Section 4: $g^\star(\log(\tau)) = \max(\log(\tau), 1)$ and $Cauchy(0, 30)$ hyperprior on $\log(\tau)$, where $\bar{x}_0 = 0$, $n_0 = 60$, $n = 30$, and fixed $\sigma^2 = \sigma_0^2 = \hat{\sigma}_0^2 = 1$. Each graph in the top row shows results for α_0, while the bottom row shows results for $\log(\tau)$. Each column corresponds to $\bar{x} = (-1.2, -0.8, -0.4, 0)$.

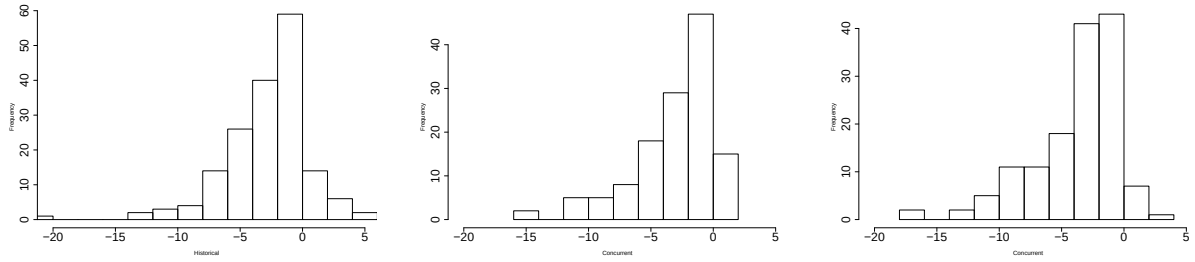

Figure 3. Histograms of average change in ld tumor sum from baseline for the colorectal cancer data used in Section 5: historical IFL (left), concurrent IFL (center), FOLFOX (right).